Cellulose (2009) 16:65–74
DOI 10.1007/s10570-008-9235-3

Indirect evidence of supramolecular changes within cellulose microfibrils of chemical pulp fibers upon drying

Eero Kontturi · Tapani Vuorinen

Received: 7 March 2008 / Accepted: 28 May 2008 / Published online: 12 June 2008

Abstract Dried and never-dried chemical pulps were subjected to strong sulfuric acid hydrolysis and the dimensions of the resulting cellulose nanocrystals (CNCs) were characterized by AFM image analysis. Although the average length of CNCs was fairly similar in all samples (55–65 nm), the length distribution histograms revealed that a higher number of longer crystals and a lower number of shorter crystals were present in the CNC suspensions prepared from never-dried pulps. The distinction was hypothetically ascribed to tensions building in individual cellulose microfibrils upon drying, resulting in irreversible supramolecular changes in the amorphous regions. The amorphous regions shaped by tensions were deemed as more susceptible to acid hydrolysis.

Keywords Cellulose microfibrils · Hornification · Nanocrystalline cellulose · Thermal drying

Introduction

A wood fiber becomes excessively porous when chemical pulping removes lignin from between the cellulose microfibrils in native wood (Stone and Scallan 1965; Maloney and Paulapuro 1999; Fahlén and Salmén 2005). As long as the pulp fiber stays in aqueous environment, these pores are filled with water, i.e., they are in a swollen state. Upon drying a pulp fiber, the water is withdrawn from between the cellulose microfibrils and, if exposed to water again, the swelling is not restored to the original level. This irreversible shrinkage of pulp fibers is called hornification, a term coined by Jayme (1944). Fiber swelling is particularly important in papermaking since the once-dried, hornified fibers are relatively stiff, resulting in paper with inferior strength properties (Higgins and McKenzie 1963; Hubbe et al. 2007; Wistara and Young 1999).

Ever since the formal definition, the fundamental facts behind hornification have been subject to conjectural curiosity (Nazhad and Paszner 1994; Fernandes Diniz et al. 2004; Laivins and Scallan 1993; Hubbe et al. 2007). It is effectively a molecular level phenomenon, something to do with the internal arrangement of cellulose microfibrils, the smallest supramolecular units of cellulose chains in native cellulosic fibers. The most credible explanations address irreversible microfibril aggregation (Hult et al. 2001) or co-crystallization (Newman 2004) but whatever the reasoning, drying is generally expected to cause something in the radial direction of the microfibrils. In this paper, we want to communicate that changes take place also in the longitudinal direction of the microfibrils when

E. Kontturi (✉) · T. Vuorinen
Department of Forest Products Technology, Helsinki University of Technology, P.O. Box 6300, 02015 TKK Helsinki, Finland
e-mail: eero.kontturi@tkk.fi

chemical pulp fibers are dried. This means supramolecular rearrangements occurring within a single cellulose microfibril in contrast to the previously reported rearrangements of cellulose microfibrils with each other. Aside a link to hornification, pulping and papermaking, the changes in single microfibrils are important in understanding the reactivity of cellulose in dried and never-dried chemical pulps. Usually the reactions are restricted in dried fibers because of the reduced accessibility in the cell wall caused by irreversible pore closure (Staudinger et al. 1942; Barzyk et al. 1997). Occasional reports, however, indicate an improved reactivity after thermal drying in, for instance, alkaline swelling (Hernadi and Dömötör 1981) or acid hydrolysis (Steege and Philipp 1974). Fundamental understanding of the heterogeneous acid hydrolysis of native cellulose helps illuminate the phenomena taking place in various other degradation processes; for example, within the present efforts to obtain glucose from lignocellulosics to produce ethanol for transportation fuels (Huber et al. 2006; Farrell et al. 2006). Furthermore, unraveling the fundamental response of native cellulose to drying and acid hydrolysis has a value in the current trend of applying native cellulose as a smart material (Kim et al. 2006) or preparing nanosized cellulosic products for materials science (Pääkkö et al. 2007; Abe et al. 2007; Andresen et al. 2007).

In this work, the supramolecular changes have been made visible indirectly by preparing cellulose nanocrystals (CNC) by acid hydrolysis from never-dried and dried chemical pulp. The CNC preparation is closely related to the level-off degree of polymerization (LODP) that represents the nearly constant value where DP of cellulose settles after a fast initial decrease during severe acid hydrolysis (Battista et al. 1956). The imaging and subsequent image analysis of the CNCs, however, yields a length distribution (Beck-Candanedo et al. 2005) whereas LODP is often employed just as a single number. Moreover, CNCs are currently gaining momentum because of their exceptional physico-chemical and material properties (Fleming et al. 2001; de Souza Lima and Borsali 2004; Azizi Samir et al. 2005). This work highlights the reciprocal relation between CNCs and their starting material in a more subtle manner than the usual considerations over the botanical source.

Experimental

Materials

Elementarily chlorine free (ECF) fully bleached softwood kraft pulp was provided by a pulp mill in Eastern Finland [90% pine (*Pinus sylvestris*), 10% spruce (*Picea abies*), according to the manufacturer; kappa number 0.7 as determined by ISO 302:2004]. Sulphuric acid was obtained as a 98% (p.a.) solution from VWR. Silicon wafers (silicon <100> with a native oxide layer on top) were purchased from Okmetic (Espoo, Finland). Titanium(IV) bis(ammonium lactato)dihydroxide was obtained as 50% aqueous solution from Aldrich.

Pulp analysis

Water retention value (WRV) of the pulps was determined according to the standard ISO 23714:2007 with a Jouan GR 4 22 centrifuge. Viscosity of the pulps was measured according to the standard ISO 5351:2004.

Pulp treatments

The never-dried reference pulp sample was subjected to three different treatments: (i) fast drying in oven at 110 °C for 12 h; (ii) gentle drying in 50% relative humidity at 25 °C for 7 days; (iii) laboratory beating in PFI mill for 4,000 revolutions (ISO 5264-2:2002). The beaten pulp was not subjected to drying before or after the treatments. The dryings applied do not correspond to industrial drying of pulp but they are considered appropriate for the initial fundamental research that is the objective of this study. Similar dryings have been previously applied in laboratory scale research on the effect of drying on pulp fibres (Laine et al. 2003).

Preparation of cellulose nanocrystals (CNCs)

The hydrolysis was performed with 64% aqueous sulphuric acid at 45 °C for 25 min at 2% consistency. These conditions were chosen because they are reportedly the optimal conditions for CNC preparation from wood pulp (Beck-Candanedo et al. 2005). Furthermore, these conditions resulted in almost identical yields and sulfur contents of the samples used (Table 1), meaning that the extent of hydrolysis should be similar in all the samples.

Table 1 Yield and sulfur content of CNCs from the analyzed samples

Sample	CNC yield (%)	Sulfur/ Carbon mass ratio	Apparent degree of substitution of sulfur[a]
Never-dried	49	0.22	0.050
Dried in 110 °C	50	0.22	0.050
Dried in RH50%	52	0.23	0.051
Never-dried, beaten	54	0.23	0.051

[a] The atomic share of sulfur per anhydroglucose unit of cellulose. Assuming that the sulfate groups are exclusively on the CNC surface, the degree of substitution of the surface chains of cellulose is ca. 0.1, which complies with the literature accounts on CNCs (Fleming et al. 2001)

Reproducible hydrolysis required great care over the conditions (time, temperature, acid concentration). In the case of never-dried pulps, the water content of the pulp was determined from the dry matter content (ISO 638:1978). Readily diluted sulphuric acid was then added dropwise over a period of 1 h into the pulp which was constantly being stirred in an ice bath so that the concentration of the sulphuric acid in the final mixture was 64%. In the case of dried pulps, first an amount of water was added to the pulp to make it the same consistency as never-dried pulp, after which the same procedure commenced as with never-dried pulp. Washing by centrifugation, purification by dialysis and individualization of the nanocrystals by ultrasonic treatment as well as purification in a mixed bed resin were performed according to Edgar and Gray (2003).

Sulfur analysis

Sulfur analysis was performed with LECO SC-444 Sulfur and Carbon analyzer (LECO, St. Joseph, Michigan). Furnace temperature was 1350 °C, pure (99.5%) oxygen was used as a combustion gas (3.5 l/min flow rate) and anhydrous $MgClO_4$ as the reagent. The elemental carbon and sulfur amounts were detected in separated IR-cells.

Submonolayers of CNCs

Submonolayers of CNCs were prepared onto titania substrates which were prepared on silica wafers from Titanium(IV) bis(ammonium lactato)dihydroxide as described by Kontturi et al. (2007). CNC suspensions were diluted to 100 mg dm^{-3} and spin coated onto titania substrates at 4,000 rpm. This method results in even distribution of individual CNCs on the titania substrate which can be easily observed by atomic force microscopy (AFM) (Kontturi et al. 2007). The even distributions of CNC submonolayers enable automated image analysis in a statistically reliable manner.

Atomic force microscopy (AFM)

Atomic force microscopy (AFM) was performed with NanoScope IIIa multimode microscope (Digital Instruments Inc., Santa Barbara) in tapping mode. The cantilever of choice was non-contact silicon NSG10 (NT-MDT, Moscow) with a typical force constant of 11.5 N/m and typical resonant frequency of 255 kHz. The radius of curvature of the tip was below 10 nm, according to the manufacturer. The tapping mode was operated with "hard tapping" by setting the set point amplitude to ~30–40% of the free-oscillating amplitude.

Image analysis

The average height of the CNCs in each 5 × 5 μm^2 image was determined from the height distribution histograms. The actual width of CNCs in AFM images is unreliable because of the finite tip dimensions but the height measurement is accurate. An example of a height distribution histogram is given in Fig. 1. The histogram consists essentially of two regimes which can be resolved using a Gaussian peak fit (performed by Origin 7.0, Microcal). The lower regime consists of the titania substrate and the higher regime from CNCs. The subtract of the center of the two Gaussians gives the average height difference between titania and CNCs (Fig. 1: $xc_{CNC} - xc_{TiO_2}$). To deduce the height of the CNCs, we have to take into account their "average roughness" (i.e., absolute height variation), given by full width at half height (FWHH) of the CNC Gaussian peak. Average height (h) of the CNCs is then given by adding FWHH/2 to the average height difference:

$$h = (xc_{CNC} - xc_{TiO_2}) + \frac{FWHH}{2}. \quad (1)$$

The h values of parallel samples were highly reproducible. The histogram analysis is necessary since the titania substrate has already a considerable

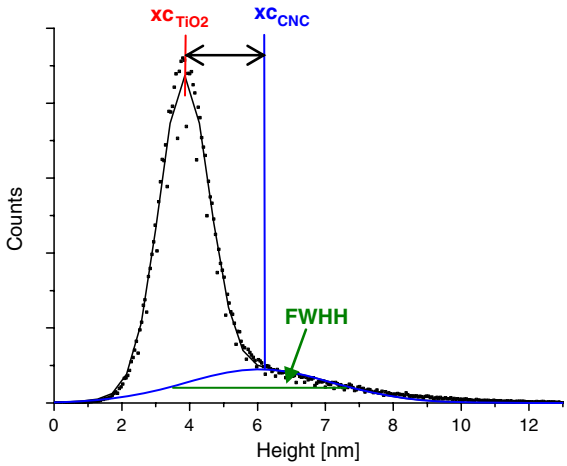

Fig. 1 Height distribution histogram of a 5 × 5 μm^2 AFM image of CNCs, prepared from never-dried pulp. The histograms can be resolved to contributions from the titania substrate (lower regime) and CNCs (higher regime) by Gaussian peak fit. Average height of the CNC contribution is given by subtracting the center of the CNC peak (xc_{CNC}) from the centre of the titania peak (xc_{TiO_2}). Average height of the CNCs is given by adding the halved average roughness (FWHH/2) to the value (Eq. 1)

roughness as opposed to, for example, smoother mica or graphite surfaces where a certain threshold can be used in the height analysis (Beck-Candanedo et al. 2005; Schneider et al. 2003).

Average length and histograms of CNC length distribution were extracted with Scanning probe image processor (SPIP) (Image Metrology, Lyngby, Denmark) by using Watershed algorithm in the Grain Analysis feature. In this algorithm, a threshold value above the roughness of the substrate and below the height of CNCs is chosen. Because the length measurement is parallel and not perpendicular to the substrate, a threshold value can be used contrary to the height determination. The length of each feature above this threshold is then taken into account. The threshold value was set to 3.5 nm from the lowest point in the image. Length, being a far larger dimension than width, is not subject to broad tip exaggeration in relative terms. The uncertainty in length measurement for CNCs with a 4 nm height is 8 nm at most (with 10 nm radius of curvature for the tip). Maximum length was calculated from each image and the value represents the average of the length of the longest CNC in parallel images with error limits originating from the absolute deviation between parallel images. For length distribution histograms, all CNC lengths from all 18 images per each sample were utilized additively.

Two batches of CNCs were prepared from each sample and three submonolayers of each batch were prepared. AFM imaging was performed on three spots on each sample, i.e., the figures from image analysis consist of an analysis of 18 images. The values extracted from image analysis (subsequently in Table 2) are presented with error limits that stem from the absolute deviation between the parallel images, i.e., the error limits are not standard deviation values which are presented separately in Table 2.

Results and discussion

Pulp analysis

Analysis of the treated pulps shows the expected trends (Table 2). Swelling of the pulps decreases

Table 2 Water retention value and viscosity results from the pulp samples and the results from dimensional analysis of CNCs prepared from the pulp samples

Sample	Water retention value (WRV) (%)	Pulp viscosity (ml/g)	Apparent height of crystals (nm)[a]	Average length of crystals (nm)[b]	Maximum length of crystals (nm)[b]	Standard deviation in length (nm)[b]
Never-dried	149	825	4.4 ± 0.2	63 ± 5	630 ± 110	53 ± 9
Dried in 110 °C	96	824	4.3 ± 0.2	53 ± 4	380 ± 40	31 ± 4
Dried in RH50%	108	845	4.0 ± 0.3	64 ± 5	360 ± 40	28 ± 4
Never-dried, beaten	183	755	4.1 ± 0.2	60 ± 5	510 ± 100	40 ± 5

The CNC dimensions are averages of parallel AFM images. The error limits in CNC dimensions correspond to absolute deviations between the average values extracted from parallel images (18 images for each sample, see Experimental section for details). AFM tip convolution accounts for maximum 8 nm exaggeration in length determination

[a] Calculated from height distribution histograms (Fig. 1)

[b] Calculated by image analysis from full length histograms provided by Scanning Probe Image Processor

irreversibly as a result of drying, which is reflected by a decrease in the water retention values (WRV) of the dried pulps. The decrease in WRV is slightly more pronounced after fast drying in high (110 °C) temperature than after gentle drying. The figures correspond well to the earlier efforts of deliberate hornification by fast and gentle drying (Matsuda et al. 1994; Laine et al. 2003). Beating was selected for the sample series because it, contrary to drying, facilitates the pore opening within the fibers. Therefore, beating expectedly increases WRV, which can indeed be explained by the pore opening, i.e., internal fibrillation (dispersion) of the cellulose microfibrils, caused by the mechanical energy (Page 1985).

The viscosity values of the pulps reflect the degree of polymerization (DP) of cellulose (da Silva Perez and van Heiningen 2002). Table 2 unequivocally exposes that no chain degradation takes place in cellulose under the applied treatments except for the slight chain scission introduced by the shear forces in PFI beating. Although 110 °C is rather a harsh temperature treatment, the stability of cellulose DP is no surprise since the occurrence of cellulose chain degradation would still require additional humidity at this temperature (Welf et al. 2005). Beating results in a slight decrease in DP which is just detectable (Table 2).

Image analysis of CNCs: height

CNC suspensions were prepared from each pulp sample under identical conditions and, subsequently, a submonolayer of CNCs was imaged by AFM and the images were exposed to image analysis. The preparation of CNCs is enabled by the structure of native cellulose: cellulose chains are arranged in longitudinal microfibrils in the fiber cell wall and within the microfibrils highly ordered crystalline domains are regularly interrupted by less ordered "amorphous" regions (this is called the fringed fibrillar theory of cellulose microfibrils; Mark 1940; Klemm et al. 2005). The amorphous domains can be hydrolyzed in a controllable fashion in strong acid hydrolysis, leaving the crystalline regions intact. The result is CNCs, needle-like nanocrystals of high aspect ratio (Fleming et al. 2001; de Souza Lima and Borsali 2004). The crystallinity of cellulose in kraft pulps is in the order of 55–70% (Liitiä et al. 2003) and the yields of CNCs in this work are around 50% (Table 1), meaning that most of the crystalline cellulose has been preserved during the acid hydrolysis.

Recently, Elazzouzi-Hafraoui et al. (2008) convincingly demonstrated that CNCs consist of several laterally parallel crystallites which have the dimensions of a microfibril. This may well be the case with the nanocrystals in this work but the height analysis of the crystallites on spin coated submonolayers leaves the question open. Spin coating has a tendency to align asymmetric particles with the side of the largest area facing the substrate (Kontturi et al. 2007), i.e., the height determination does not reveal whether a CNC has several crystallites in parallel alignment with each other. Moreover, the tip convolution of AFM means that the width of CNCs cannot be accurately measured (Kvien et al. 2005). This is why the discussion here is limited to the height of CNCs.

Figure 2 shows representative AFM images of CNC submonolayers from each sample. The first observation from image analysis is that the height of the CNCs is virtually the same in all of the samples (Table 2). This correlates with solid state NMR

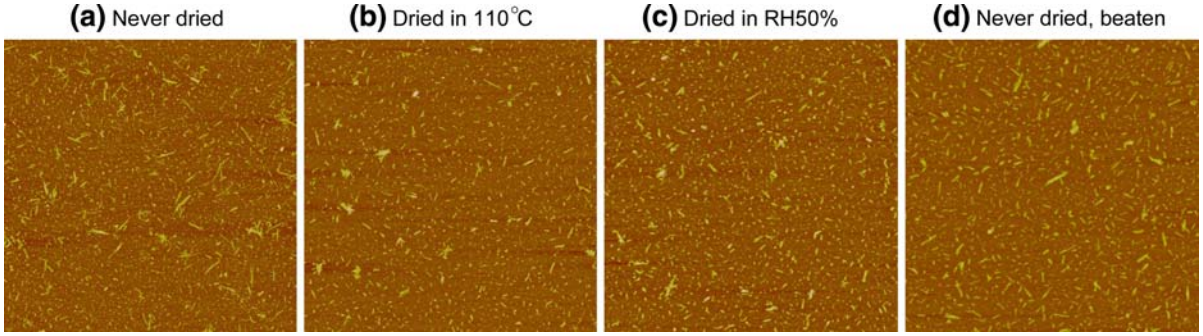

Fig. 2 5 × 5 μm^2 AFM height images of CNC submonolayers, prepared from (**a**) never- dried pulp, (**b**) pulp dried in 110 °C for 12 h, (**c**) pulp dried in 50% relative humidity for 7 days, and (**d**) pulp beaten in PFI mill for 4,000 revolutions

results of individual microfibril dimensions from dried and never-dried pulps (Hult et al. 2001; Rebuzzi and Evtuguin 2006). To our knowledge, CNC dimensions from never-dried pulp have never been reported before.

Also beating does not induce changes in the CNC height (Table 2). This is in correlation with the NMR studies by Hult et al. (2002) who found that the microfibril dimensions of kraft pulp fibers were unchanged after beating.

As for the absolute values of CNC height, they vary between 3.7 and 4.6 nm within the samples (Table 2). The values are slightly (ca. 0.5 nm) lower than the ones described by Beck-Candanedo et al. (2005) for CNCs from eucalyptus and black spruce chemical pulps. Similarly to these experiments, the authors applied AFM image analysis of CNCs deposited on smooth surfaces and measured the height of CNCs. Therefore, the small difference may be due to the different nature of height determination from height distribution histograms in this work (Fig. 1) or AFM measurement parameters. The difference in wood species, which the pulp was originally prepared from, may also influence the CNC width. On the other hand, the CNC heights in this work are slightly higher than the widths reported by Araki et al. (1998) whose electron microscopy analysis gave a width of 3.5 nm for CNCs prepared from bleached softwood kraft pulp. They did not, however, perform any wider statistical survey on the CNC dimensions.

As postulated already by Rånby (1951), CNC preparation corresponds to individualization of the crystalline segments of cellulose microfibrils. According to the fringed fibrillar model (Klemm et al. 2005), the crystalline segments are separated in the longitudinal direction by amorphous segments; in other words, the height of CNCs should essentially be similar to the width of a cellulose microfibril. The heights in this study (Table 2) correlate fairly well with the microfibril width determinations from kraft pulp by NMR (Hult et al. 2001; Rebuzzi and Evtuguin 2006) or X-ray diffraction (Fink et al. 1990).

Image analysis of CNCs: length

A straightforward unexpected observation is the small average length of CNCs: 55–65 nm for all samples (Table 2). Araki et al. (1998) reported an average length of 180 ± 75 nm for CNCs from bleached softwood kraft pulp, as discerned from TEM images. Beck-Candanedo et al. (2005) performed a wider statistical analysis from AFM images and ended up with 140 ± 6 nm length (standard deviation 60 nm) for CNCs prepared from bleached softwood kraft pulp under conditions similar ours. The AFM samples by Beck-Candanedo et al. (2005) were prepared by adsorption from CNC suspensions onto mica. Since both the CNCs and the mica surface are anionic, the CNC submonolayer distributions may have been influenced by the electrostatic effects during adsorption. One can speculate that the smallest CNCs are likely to be the most hydrolyzed ones, including the highest amount of sulfate groups. It is logical that these highly anionic short CNCs are the least likely CNCs to adsorb on an anionic mica surface, resulting in a distribution of greater lengths in the dimensional analysis. In the case of our samples, the shorter CNCs with a higher anionic charge are more likely to adsorb on cationic titania during spin coating (Kontturi et al. 2007). The electrostatic attraction between the CNCs and the substrate may also overemphasize the number of smaller CNCs, provided that the speculation on the higher charge of smaller CNCs is correct. The present study is, however, focused on the dimensional differences of CNCs prepared from dried and never-dried pulps. Additionally, the average lengths of the CNCs in Table 2 are extracted from 18 AFM images (>10,000 individual CNCs), amounting to a higher sampling number than with most published works on CNCs.

Interestingly, in his seminal study Rånby (1951) reported an average length of 46 nm for CNCs from bleached sulfite pulp prepared by hydrolysis in 2.5 N boiling sulfuric acid for 6 h. Furthermore, our average lengths of 55–65 nm (Table 2) correspond to a DP value of ca. 110–120, presuming that a cellobiose unit in native crystalline cellulose is regarded as ca. 1.03–1.04 nm long (for both allomorphs, cellulose I_α and I_β; Davidson et al. 2004). One hundred and twenty is close to the reported LODP values of kraft pulp (that range between 100 and 190) (Battista et al. 1956; Rebuzzi and Evtuguin 2006; Unger et al. 1995). In addition, recent evidence suggests that LODP does correspond to the periodicity of the disordered (called here amorphous) regions in a native cellulose microfibril (Nishiyama et al. 2003), i.e., the length of the crystalline segment. However,

almost all of the recent studies on CNCs report categorically higher average lengths (Beck-Candanedo et al. 2005; Fleming et al. 2001; de Souza Lima and Borsali 2004; Araki et al. 1998) than the corresponding LODP values (Battista et al. 1956; Rebuzzi and Evtuguin 2006; Unger et al. 1995). Perhaps one way to view CNC preparation may be as an interrupted form of LODP determination.

In contrast to the relatively unchanged width of the CNCs upon the selected treatments, a cursory glance at the AFM images of Fig. 2 reveals obvious distinctions in their length distribution. Although the average length varies little between the samples (because of the large amount of very short CNCs in every sample), there are sharp dissimilarities in the maximum length of the CNCs (Table 2). The longest CNCs prepared from never-dried fibers—also from the beaten ones—are over 60% longer than those prepared from dried pulps. Since the number of CNCs which are in the order of the maximum length is very small in each image, the distinction is made statistically more credible in CNC length distribution histograms (Fig. 3). We emphasize that the images are fully representative, i.e., the counts in each histogram originate additively from 18 parallel AFM images of 2 parallel CNC samples (see Experimental section). Moreover, the batch-to-batch variability between the CNCs of parallel samples is smaller than the variability between parallel images (data not shown), highlighting the reproducibility of the sample preparation. It is evident that drying, especially thermal drying, prior to CNC preparation results in a higher number of short CNCs and, in particular, a lower number of long CNCs. In other words, dried fibers are more susceptible to acid hydrolysis than never-dried ones. A similar observation was actually made over 30 years ago in the case of dried and never-dried beech sulfite pulp: it took twice the amount of time for never-dried pulp to reach the LODP compared to dried pulp in identical hydrolysis conditions (Steege and Philipp 1974). Regrettably, however, the authors did not elaborate on the possible reasons behind this rather surprising result.

Between thermally and gently dried pulp, a slight difference exists in the length distribution histograms, with a higher amount of longer crystals in the gently dried sample in RH50% (Fig. 3). This is consistent with the extent of hornification which is reportedly greater upon harsh thermal drying compared with

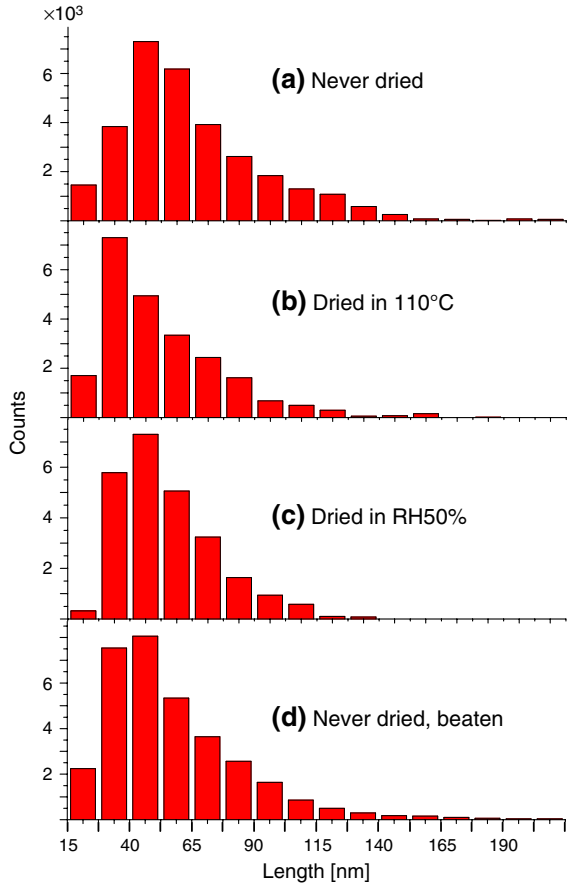

Fig. 3 Length distribution histograms (up to 215 nm length) of CNCs prepared from (**a**) never-dried pulp, (**b**) pulp dried in 110 °C for 12 h, (**c**) pulp dried in 50% relative humidity for 7 days, and (**d**) pulp beaten in PFI mill for 4,000 revolutions. Each histogram has been additively derived from 18 individual images (see Experimental section)

gentle drying (Laine et al. 2003). However, the comparison of CNC dimensions from differently dried pulps does not reveal drastic differences and, for example, the maximum lengths of CNCs are similar for both samples (Table 2).

Cellulose crystallinity upon drying is generally reported to be negligible (Matsuda et al. 1994) or minutely increased (Newman 2004; Rebuzzi and Evtuguin 2006). Moreover, chemical changes during drying should be minimal: the DP of cellulose stays the same (viscosity values, Table 2) and the possible alterations (Röder and Sixta 2004) in the small amounts of hemicellulose should not affect the acid hydrolysis as they are removed at an early stage of the process. Even when the small change in crystallinity of cellulose is taken into consideration, it should hinder

the course of hydrolysis, not facilitate its progress. Figure 3 reveals, nevertheless, that the hydrolysis is more efficient on the dried fibers because of a higher amount of very short CNCs and a lower amount of long CNCs. We make now three literature-based assumptions: (i) the fringed fibrillar theory of altering crystalline and amorphous segments in a native cellulose microfibrils is correct (Klemm et al. 2005), (ii) acid hydrolysis targets mainly the amorphous (or disordered) regions in a microfibril (Battista et al. 1956; Rånby 1951; Nishiyama et al. 2003), and (iii) drying does not affect the length of the crystalline region in a microfibril [drying does not change the LODP of chemical pulp fibres (Steege and Philipp 1974)]. Based on these assumptions, we conclude that there are more amorphous segments in dried fibers which are more susceptible to acid hydrolysis than there are in never-dried fibers. Therefore, we hypothetically propose that drying induces supramolecular changes within the amorphous sections in cellulose microfibrils.

The proposed supramolecular changes in cellulose microfibrils are not a cause for fiber stiffening during hornification but rather a result of it. As the partially irreversible microfibril aggregation occurs during drying (Laivins and Scallan 1993; Hult et al. 2001), the rearrangement causes tensions in the microfibrils due to the finite dimensions of the cell wall, amounting to stress in the microfibrils. [The tension is reflected by a well-known increase in the elastic modulus of fibers upon drying. (Scallan and Tigerström 1992)] Stress in amorphous cellulose leads to supramolecular rearrangements in the hydrogen bonding network, according to molecular modeling (Chen et al. 2004). The rearrangements leave the amorphous segments in a higher energetic state, thus rendering them more susceptible to acid hydrolysis than before the stress (i.e., in never-dried state). It is only natural that the stress in the amorphous region is more pronounced after the fast water removal of thermal drying, resulting in a more efficient acid hydrolysis with shorter CNCs (Fig. 3b). Furthermore, the stress in the amorphous regions does not disappear as the fiber is wetted before hydrolysis because of the irreversible nature of hornification: portions of microfibrils are associated with each other and remain so in the wet state (Nazhad and Paszner 1994; Fernandes Diniz et al. 2004; Laivins and Scallan 1993; Hult et al. 2001; Newman 2004; Hubbe et al. 2007). Usually the irreversible aggregation of microfibrils in hornification renders the fibers less reactive because the accessibility, i.e., surface area of the fiber, has been reduced (Staudinger et al. 1942; Barzyk et al. 1997; Laine et al. 2003). However, in those cases where the reaction occurs predominantly in the amorphous segment of the microfibril, the reduced accessibility is overshadowed by the stress in amorphous cellulose and the fiber becomes more reactive. Acid hydrolysis is such reaction, as shown in this work and in the earlier work of Steege and Philipp (1974). Proper quantitative treatment on the acid hydrolysis of dried and never-dried pulp fibers would require kinetic studies and it is outside the scope of this introductory paper.

Although 64% sulfuric acid hydrolysis is industrially insignificant with lignocellulosics, the results here help understand better the heterogeneous degradation of native cellulose, which is increasingly important, for example, in the current efforts to produce bioethanol from cellulosic sources (Huber et al. 2006; Farrell et al. 2006). Another field which may benefit from the current results is materials science where, for example, the recent reintroduction of cellulose as smart material is largely based on the altering crystalline/amorphous regions in a microfibril (Kim et al. 2006). The tension hypothesis of amorphous regions, alongside other hornification artifacts, should be considered when designing such niche applications from cellulose. Furthermore nanosized cellulosic materials have recently been widely reported (Pääkkö et al. 2007; Abe et al. 2007; Andresen et al. 2007) and at least their preparation may well be influenced by the supramolecular changes in amorphous regions presented in this paper.

Conclusions

By preparing cellulose nanocrystals (CNCs) of never-dried and dried pulps, we have shown that CNC preparation can be used as an analytical tool to see actual contrasts in dried and never-dried fibers.

We propose the following hypothetical conclusions:

1. Heterogeneous acid hydrolysis of chemical pulp fibers can be influenced by simple drying of the starting material.

2. Acid hydrolysis is facilitated by drying the fibers beforehand, especially by thermal drying in 110 °C.
3. Hypothetically, the irreversible aggregation of cellulose microfibrils during drying causes tensions, i.e., forced supramolecular changes, in the amorphous regions of the microfibrils. The tense amorphous regions are more susceptible to acid hydrolysis
4. Modern CNC preparation may be seen as an interrupted form of level-off degree of polymerization (LODP) determination.

Acknowledgements The authors thank Mr. Timo Pääkkönen for laboratory assistance. Dr. Juha Linnekoski at the Department of Chemistry (TKK) is acknowledged for performing the sulfur analysis. The Finnish Funding Agency for Technology and Innovation (TEKES) as well as Andritz, UPM-Kymmene, Kemira, Metso, and M-real corporations are acknowledged for the financial support.

References

Abe K, Iwamoto S, Yano H (2007) Obtaining cellulose nanofibers with a uniform width of 15 nm from wood. Biomacromolecules 8:3276–3278. doi:10.1021/bm700624p

Andresen M, Stenstad P, Møretrø T, Langsrud S, Syverud K, Johansson L-S et al (2007) Nonleaching antimicrobial films prepared from surface-modified microfibrillated cellulose. Biomacromolecules 8:2149–2155. doi:10.1021/bm070304e

Araki J, Wada M, Kuga S, Okano T (1998) Flow properties of microcrystalline cellulose suspension prepared by acid treatment of native cellulose. Colloids Surf A Physicochem Eng Asp 142:75–82. doi:10.1016/S0927-7757(98)00404-X

Azizi Samir MAS, Alloin F, Dufresne A (2005) Review of recent research into cellulosic whiskers, their properties and their application in nanocomposite field. Biomacromolecules 6:612–626. doi:10.1021/bm0493685

Barzyk D, Page DH, Ragauskas A (1997) Acidic group topochemistry and fiber-to-fiber specific bond strength. J Pulp Pap Sci 23:J59–J61

Battista OA, Coppick S, Howsmon JA, Morehead FF, Sisson WA (1956) Level-off degree of polymerization. Ind Eng Chem 48:333–335. doi:10.1021/ie50554a046

Beck-Candanedo S, Roman M, Gray DG (2005) Effect of reaction conditions on the properties and behavior of wood cellulose nanocrystal suspensions. Biomacromolecules 6:1048–1054. doi:10.1021/bm049300p

Chen W, Lickfield G, Yang CQ (2004) Molecular modeling of cellulose in amorphous state. Part I: model building and plastic deformation study. Polymer (Guildf) 45:1063–1071. doi:10.1016/j.polymer.2003.11.020

da Silva Perez D, van Heiningen ARP (2002) Determination of cellulose degree of polymerization in chemical pulps by viscosimetry. In: Seventh European workshop on lignocellulosics and pulp: proceedings. Åbo Akademi, Turku, pp 393–396

Davidson TC, Newman RH, Ryan MJ (2004) Variations in the fibre repeat between samples of cellulose I from different sources. Carbohydr Res 339:2889–2893. doi:10.1016/j.carres.2004.10.005

de Souza Lima MM, Borsali R (2004) Rodlike cellulose microcrystals: structure, properties, and applications. Macromol Rapid Commun 25:771–787. doi:10.1002/marc.200300268

Edgar CD, Gray DG (2003) Smooth cellulose I surfaces from nanocrystal suspensions. Cellulose 10:299–306. doi:10.1023/A:1027333928715

Elazzouzi-Hafraoui S, Nishiyama Y, Putaux J-L, Heux L, Dubreuil F, Rochas C (2008) The shape and size distribution of crystalline nanoparticles prepared by acid hydrolysis of native cellulose. Biomacromolecules 9:57–65. doi:10.1021/bm700769p

Fahlén J, Salmén L (2005) Pore and matrix distribution in the fiber wall revealed by atomic force microscopy and image analysis. Biomacromolecules 6:433–438. doi:10.1021/bm040068x

Farrell AE, Plevin RJ, Turner BT, Jones AD, O'Hare M, Kammen DM (2006) Ethanol can contribute to energy and environmental goals. Science 311:506–508. doi:10.1126/science.1121416

Fernandes Diniz JMB, Gil MH, Castro JAAM (2004) Hornification—its origin and interpretation in wood pulps. Wood Sci Technol 37:489–494. doi:10.1007/s00226-003-0216-2

Fink HP, Hofmann D, Purz HJ (1990) Zur Fibrillarstruktur nativer cellulose. Acta Polym 41:131–137. doi:10.1002/actp. 1990.010410213

Fleming K, Gray DG, Matthews S (2001) Cellulose crystallites. Chem Eur J 7:1831–1835. doi:10.1002/1521-3765(20010504)7:9<1831::AID-CHEM1831>3.0.CO;2-S

Hernadi A, Dömötör J (1981) Water take-up and swelling of cellulose fibers after thermal treatment. Cellulose Chem Technol 15:63–75

Higgins HG, McKenzie AW (1963) The structure and properties of paper XIV. Effects of drying cellulose fibers and the problem of maintaining pulp strength. Appita 16:145–164

Hubbe MA, Vendetti R, Rojas OJ (2007) What happens to cellulosic fibers during papermaking and recycling? A review. BioResources 2:739–788

Huber GW, Iborra S, Corma A (2006) Synthesis of transportation fuels from biomass: chemistry, catalysts and engineering. Chem Rev 106:4044–4098. doi:10.1021/cr068360d

Hult E-L, Larsson PT, Iversen T (2001) Cellulose fibril aggregation—an inherent property of kraft pulps. Polymer (Guildf) 42:3309–3314. doi:10.1016/S0032-3861(00)00774-6

Hult E-L, Liitiä T, Maunu SL, Hortling B, Iversen T (2002) A CP/MAS ^{13}C-NMR study of cellulose structure on the surface of refined kraft pulp fibers. Carbohydr Polym 49:231–234. doi:10.1016/S0144-8617(01)00309-5

Jayme G (1944) Mikro-Quellungsmessungen an Zellstoffen. Papier-Fabrikant/Wochenblatt für Papierfabrikation 42:187–194

Kim J, Yun S, Ounaies Z (2006) Discovery of cellulose as a smart material. Macromolecules 39:4202–4206. doi:10.1021/ma060261e

Klemm D, Heublein B, Fink H-P, Bohn A (2005) Cellulose: fascinating biopolymer and sustainable raw material. Angew Chem Int Ed 44:3358–3393. doi:10.1002/anie.200460587

Kontturi E, Johansson L-S, Kontturi KS, Ahonen P, Thüne PC, Laine J (2007) Cellulose nanocrystal submonolayers by spin coating. Langmuir 23:9674–9680. doi:10.1021/la701262x

Kvien I, Tanem BS, Oksman K (2005) Characterization of cellulose whiskers and their nanocomposites by atomic force microscopy and electron microscopy. Biomacromolecules 6:3160. doi:10.1021/bm050479t

Laine J, Lindström T, Bremberg C, Glad-Nordmark G (2003) Studies on topochemical modification of cellulosic fibres. Part 4: toposelectivity of carboxymethylation and its effects on the swelling of fibres. Nord Pulp Pap Res J 18:316–324. doi:10.3183/NPPRJ-2003-18-03-p316-324

Laivins GV, Scallan AM (1993) The mechanism of hornification of wood pulps. In: Baker CF (ed) Products of papermaking: transactions of the 10th fundamental research symposium held at Oxford, vol 2. Pira International, Leatherhead, pp 1235–1260 September 1993

Liitiä T, Maunu SL, Hortling B, Tamminen T, Pekkala O, Varhimo A (2003) Cellulose crystallinity and ordering of hemicelluloses in pine and birch pulps as revealed by solid-state NMR spectroscopic methods. Cellulose 10:307–316. doi:10.1023/A:1027302526861

Maloney TC, Paulapuro H (1999) The formation of pores in the cell wall. J Pulp Pap Sci 25:430–436

Mark H (1940) Intermicellar hole and tube system in fiber structure. J Phys Chem 44:764–788. doi:10.1021/j150402a009

Matsuda Y, Isogai A, Onabe F (1994) Effects of thermal and hydrothermal treatments on the reswelling capabilities of pulps and paper sheets. J Pulp Pap Sci 20:J323–J327

Nazhad MM, Paszner L (1994) Fundamentals of strength loss in recycled paper. Tappi J 77:171–179

Newman RH (2004) Carbon-13 NMR evidence for cocrystallization of cellulose as a mechanism for hornification of bleached kraft pulp. Cellulose 11:45–52. doi:10.1023/B:CELL.0000014768.28924.0c

Nishiyama Y, Kim U-J, Kim D-Y, Katsumata KS, May RP, Langan P (2003) Periodic disorder along ramie cellulose microfibrils. Biomacromolecules 4:1013–1017. doi:10.1021/bm025772x

Pääkkö M, Ankerfors M, Kosonen H, Nykänen A, Ahola S, Österberg M et al (2007) Enzymatic hydrolysis combined with mechanical shearing and high-pressure homogenization for nanoscale cellulose fibrils and strong gels. Biomacromolecules 8:1934–1941. doi:10.1021/bm061215p

Page DH (1985) The mechanism of strength development of dried pulps by heating. Sven Papperstidn 88:R30–R35

Rånby BG (1951) The colloidal properties of cellulose micelles. Discuss Faraday Soc 11:158–164. doi:10.1039/df9511100158

Rebuzzi F, Evtuguin DV (2006) Effect of glucuronoxylan on the hornification of *Eucalyptus globulus* bleached pulps. Macromol Symp 232:121–128. doi:10.1002/masy.200551414

Röder T, Sixta H (2004) Thermal treatment of cellulose pulps and its influence to cellulose reactivity. Lenzinger Ber 83:79–83

Scallan AM, Tigerström AC (1992) Swelling and elasticity of the cell walls of pulp fibres. J Pulp Pap Sci 18:J188–J193

Schneider M, Brinkmann M, Möhwald H (2003) Adsorption of polyethyleneimine on graphite: an atomic force microscopy study. Macromolecules 36:9510–9518. doi:10.1021/ma0345293

Staudinger H, Dohle W, Heick O (1942) Über topochemische Reaktionen der cellulose. J Prakt Chem 161:191–218. doi:10.1002/prac.19431610803

Steege H-H, Philipp B (1974) Herstellung, Charakterisierung und Anwendung mikrokristalliner Zellulose. Zellst Pap 23:68–73

Stone JE, Scallan AM (1965) Effect of component removal upon the porous structure of the cell wall of wood. J Polym Sci C 11:13–25

Unger E-W, Fink H-P, Philipp B (1995) Morphometrische Untersuchung des Quell- und Lösevorgangs von Cellulosefasern in EWNN und LiCl/Dimethylacetamid. Papier 49:297–307

Welf ES, Venditti RA, Hubbe MA, Pawlak JJ (2005) The effects of heating without water removal and drying on the swelling as measured by water retention value and degradation as measured by intrinsic viscosity of cellulose papermaking fibers. Prog Pap Recycling 14:5–13

Wistara N, Young RA (1999) Properties and treatments of pulps from recycled paper. Part I: physical and chemical properties of pulps. Cellulose 6:291–324. doi:10.1023/A:1009221125962